

# Constraints on the ultraviolet metagalactic emissivity using the Ly $\alpha$ forest

Avery Meiksin<sup>1\*</sup> and Martin White<sup>2</sup>

<sup>1</sup>*Institute for Astronomy, University of Edinburgh, Blackford Hill, Edinburgh EH9 3HJ*

<sup>2</sup>*Departments of Astronomy and Physics, University of California, Berkeley, CA 94720, USA*

Accepted 2003 March 11. Received 2003 March 7; in original form 2002 December 6

## ABSTRACT

Numerical hydrodynamical simulations have proven a successful means of reproducing many of the statistical properties of the Ly $\alpha$  forest as measured in high redshift quasar spectra. The source of ionization of the intergalactic medium (IGM), however, remains unknown. We investigate how the Ly $\alpha$  forest may be used to probe the nature of the sources. We show that the attenuation of Lyman continuum photons by the IGM depends sensitively on the emissivity of the sources, permitting a strong constraint to be set on the required emissivity to match the measured values of the mean IGM Ly $\alpha$  optical depth. We find that, within the observational errors, quasi-stellar object (QSO) sources alone are able to account for the required ultraviolet (UV) background at  $z \gtrsim 4$ . By contrast, the emissivity of Lyman-break galaxies (LBGs) must decline sharply with redshift, compared with the estimated emissivity at  $z \approx 3$ , so as not to overproduce the UV background and drive the mean Ly $\alpha$  optical depth to values that are too low. We also investigate the effect of fluctuations in the UV background, as would arise if QSOs dominated. To this end, we derive the distribution function of the background radiation field produced by discrete sources in an infinite universe, including the effects of attenuation by an intervening absorbing medium. We show that, for  $z \gtrsim 5$ , the fluctuations significantly boost the mean Ly $\alpha$  optical depth, and so increase the estimate for the mean ionization rate required to match the measured mean Ly $\alpha$  optical depths. The fluctuations will also result in large spatial correlations in the ionization level of the IGM. We show that the large mean Ly $\alpha$  optical depth measured at  $z \approx 6$  suggests such large correlations will be present if QSOs dominate the UV background. A secondary, smaller effect of the UV background fluctuations is a distortion of the pixel flux distribution. While the effect on the distribution may be too small to detect with existing telescopes, it may be measurable with the extremely large telescopes planned for the future. We also show that if QSOs dominate the UV background at  $z \approx 6$ , then they will be sufficient in number to rejuvenate the ionization of a previously ionized IGM if it has not yet fully recombined.

**Key words:** methods: numerical – intergalactic medium – quasars: absorption lines.

## 1 INTRODUCTION

Numerical simulations of structure formation in the universe, incorporating hydrodynamics in cold dark matter (CDM) dominated cosmologies, have proven very successful in reproducing the statistical properties of the Ly $\alpha$  forest as measured in high redshift quasi-stellar object (QSO) spectra (Cen et al. 1994; Zhang, Anninos & Norman 1995; Hernquist et al. 1996; Zhang et al. 1997; Bond & Wadsley 1997; Theuns, Leonard & Efstathiou 1998a). The high level of statistical agreement, as high as a few per cent in the cumulative spectral flux distributions (Meiksin, Bryan & Machacek

2001), suggests that the models are capturing the essential physical nature of these highly ionized absorbing structures.

Still unknown is the nature of the sources of photoionization. The most likely candidates are photoionization by QSOs and stars in young forming galaxies or globular clusters. Estimates of the ultraviolet (UV) background required to reproduce the measured Ly $\alpha$  optical depths of the Ly $\alpha$  forest while staying within the nucleosynthesis bounds of the cosmic baryon density agree within a factor of a few with estimates of the QSO contribution to the UV background (Meiksin et al. 2001). This suggests that QSO sources contribute significantly to the UV background, and may even dominate over all other sources. A contribution will also arise from star-forming galaxies at  $z > 3$ , from which Lyman-continuum photons have been detected (Steidel, Pettini & Adelberger 2001). The total

\*E-mail: aam@roe.ac.uk

contribution from QSOs, or active galactic nuclei (AGN) more generally, and star-forming galaxies, however, remains uncertain because of the flux limitations of the surveys that detect them at these high redshifts. Generally, only the brightest sources enter the surveys, leaving the possibility of a large contribution that has gone undetected. Distinguishing the relative contributions of young stars versus AGN is thus not possible based solely on the average detected contributions of each to the UV metagalactic background.

The discreteness of the sources presents an opportunity for distinguishing between the possible natures of the dominant sources. If star-forming galaxies or globular star clusters contribute a comparable amount or more of ionizing photons to the metagalactic background as do QSO sources, then they must have a much higher spatial density than QSOs because of their relatively weaker individual luminosities. The resulting UV background would then be fairly homogeneous, except for local modulations arising from the large-scale structure of their spatial distribution. By contrast, large fluctuations in the UV background are expected at high redshifts ( $z \gtrsim 4$ ) if QSO sources dominate the background because of the rapidly growing optical depth of the intergalactic medium (IGM) to Lyman continuum photons and the rapidly diminishing number density of QSO sources (Zuo 1992a). The fluctuations in the QSO contribution will become particularly pronounced at  $z > 5$ , where the mean Ly $\alpha$  optical depth exceeds unity (Fan et al. 2001b; Becker et al. 2001), as we show here.

The role of fluctuations in the UV background on the absorption properties of the Ly $\alpha$  forest have been largely unexplored (but see Croft et al. 2002). In this paper, we investigate the effect of the fluctuations on the 1-pt flux distribution of the Ly $\alpha$  forest. We examine the effect of the background fluctuations on the power spectrum of the Ly $\alpha$  forest in a companion paper (Meiksin & White, in preparation). We base the contributions of the QSOs to the UV background and its fluctuations on the QSO luminosity functions obtained by the two degree field (2dF) survey (Boyle et al. 2000) and the Sloan Digital Sky Survey (SDSS) (Fan et al. 2001a,b, 2003).

Because of the large computational overhead in incorporating proper hydrodynamics into an  $N$ -body code, we perform simulations of the Ly $\alpha$  forest using a pure gravitational particle-mesh  $N$ -body code (PM simulations). These simulations have been shown to agree well with the full hydrodynamics computations (Meiksin & White 2001), and have the advantages of permitting both larger simulations to be run as well as greater numbers of them. Ultimately, a detailed comparison with the data will require solving the full set of hydrodynamics equations.

This paper is organized as follows. In Section 2, we discuss our simulations of the Ly $\alpha$  forest and model assumptions. Estimates of the metagalactic emissivity are given in Section 3. We derive the distribution function for the UV background fluctuations in Section 4. In Section 5 we discuss the pixel flux distribution, and finally we summarize our results in Section 6.

## 2 THE SIMULATIONS AND MODELS

### 2.1 Particle-mesh simulations

We generate spectra of the Ly $\alpha$  forest from pure dark matter simulations, mimicking the temperature of the gas using a polytropic equation of state. Comparisons with full hydrodynamics simulations show that simulations recover the principal spectral properties of the Ly $\alpha$  forest to an accuracy of 10 per cent or better in the cumulative distributions of flux, wavelet coefficients, H I column density, and Doppler parameter (Meiksin & White 2001).

The evolution of the (dark) matter is computed using a parallel implementation of a PM code. The computational volume is chosen to be periodic with side length  $l$ , and we take as our time coordinate the log of the scale factor,  $\log a$ , where  $a \equiv (1+z)^{-1}$ . Velocities are measured in units of the expansion velocity across the box  $aHL_{\text{box}}$  of comoving side  $L_{\text{box}}$ , where  $H$  is the Hubble parameter fixed by the Friedmann equation

$$H^2 \equiv H_0^2 \left( \frac{\Omega_M}{a^3} + \Omega_\Lambda + \frac{\Omega_K}{a^2} \right) \quad (1)$$

in terms of the Hubble constant  $H_0$  and the densities in matter ( $\Omega_M$ ), cosmological constant ( $\Omega_\Lambda$ ) and curvature ( $\Omega_K$ ), in units of the critical density. The density is defined from the particle positions by assigning particles to a regular Cartesian grid using the cloud-in-cell (CIC) scheme (Hockney & Eastwood 1988). The Fourier transform is taken and the force computed using the kernel  $\tilde{k}/k^2$ . We use a second-order leapfrog method to integrate the equations. The relevant positions are predicted at a half time-step and used to calculate the accelerations which modify the velocities. The time-step is dynamically chosen as a small fraction of the cell crossing time with a maximum size of  $\Delta \log a = 2$  per cent.

The initial conditions were created by displacing the particles from a uniform grid using the Zel'dovich approximation. The initial conditions were Gaussian; however, to avoid large fluctuations between different realizations we only accepted those whose low- $k$  modes closely tracked the 'mean'.

Given a set of final particle positions and velocities, we compute the spectra as follows. First, the density and density-weighted line-of-sight velocity are computed on a grid (using CIC interpolation as above) and Gaussian smoothed using fast Fourier transform (FFT) techniques in order to adequately sample the velocity field. This forms the fundamental data set. A regular grid of  $32 \times 32$  sightlines is drawn through the box, parallel to the box sides. Along each sightline we integrate (in real space) to find  $\tau(u)$  at a given velocity  $u$ . Specifically we define

$$\tau(u) = \int dx A(x) \left[ \frac{\rho(x)}{\bar{\rho}} \right]^2 T(x)^{-0.7} b^{-1} e^{-(u-u_0)^2/b^2} \quad (2)$$

where  $u_0 = xaHL_{\text{box}} + v_{\text{los}}$  and  $b = \sqrt{2k_B T/m_H}$  is the Doppler parameter, where  $m_H$  is the mass of a hydrogen atom. The flux at velocity  $u$  is  $\exp(-\tau)$ . The integration variable  $x$  indicates the distance along the box in terms of the expansion velocity across the box. In terms of the baryon density parameter  $\Omega_b$ , hydrogen baryonic mass fraction  $X$ , the metagalactic photoionization rate  $\Gamma_{-12}$ , in units of  $10^{-12}$  photons  $\text{s}^{-1}$ , and the number  $f_e$  of electrons per hydrogen nucleus, the coefficient  $A$  is given by

$$A(x) = 18.0 f_e \left( \frac{X}{0.76} \right)^2 \left( \frac{\Omega_b h^2}{0.02} \right)^2 \Gamma_{-12}^{-1}(x) L_{\text{box}} (1+z)^5, \quad (3)$$

where  $L_{\text{box}}$  is in Mpc and  $b$  in equation (2) is in  $\text{km s}^{-1}$ . The explicit  $x$  dependence of  $A$  accounts for any spatial fluctuations in the background ionization rate  $\Gamma_{-12}(x)$ . The electron fraction is given by  $f_e = 1 + (1-X)/(2X) \approx 1.16$  ( $X = 0.76$ ) for fully ionized helium, and  $f_e = 1 + (1-X)/(4X) \approx 1.08$  if the helium is only singly ionized, a possibility at the high redshifts we consider. We adopt  $f_e = 1.1$  for simplicity, noting that a different value for  $f_e$  is effectively absorbed into the ionization rate.

In the absence of UV background fluctuations,  $A$  is constant and is iteratively adjusted to obtain a pre-defined  $\bar{\tau}_\alpha \equiv -\log(\langle \exp(-\tau) \rangle)$ . To account for a fluctuating UV background field, we replace  $A$  by  $A_{-12}/[\Gamma_{S,-12} + \bar{\Gamma}_{\text{QSO},-12}(1 + \delta_{\text{QSO}})]$ , where  $\bar{\Gamma}_{\text{QSO},-12}$  is the average photoionization rate produced by the QSO sources, in units of

$10^{-12} \text{ s}^{-1}$ ,  $A_{-12}$  is the value of  $A$  for  $\Gamma_{-12} = 1$ , and  $\delta_{\text{QSO}}$  accounts for the spatial fluctuations in the QSO contribution. The values for  $\delta_{\text{QSO}}$  are drawn randomly from the distribution functions for the background intensity derived below. We consider two cases for the sources of the UV background. In the first, we assume the only sources are QSOs, so that  $\Gamma_{\text{S}} = 0$ . In the second, we allow for a smooth component  $\Gamma_{\text{S}}$  to the UV background. This component is partly present due to the re-radiation of ionizing photons through recombination in the Ly $\alpha$  forest itself, at a level by as much as  $(\alpha_{\Lambda} - \alpha_{\text{B}})/\alpha_{\Lambda} \approx 40$  per cent of the QSO contribution (Meiksin & Madau 1993; Haardt & Madau 1996). Because of structure in the Ly $\alpha$  forest, the re-radiated component also fluctuates. We neglect this contribution to the fluctuations as they likely will be less than the direct contribution from QSOs. Other possible contributions to the ionizing background include galaxies, such as LBGs, and smaller stellar systems such as intergalactic star clusters. In this case, the value of  $\Gamma_{\text{S}}$  is iterated until agreement with  $\bar{\tau}_{\alpha}$  is found.

In evaluating equation (2) we assume a power-law relation between the gas density and temperature

$$T \equiv T_0 \left( \frac{\rho}{\bar{\rho}} \right)^{\gamma-1}. \quad (4)$$

In practice,  $T_0$  and  $\gamma$  will depend on the reionization history of the IGM, but we fix  $T_0 = 2 \times 10^4 \text{ K}$  and  $\gamma = 1.5$  throughout for most of our models. The value we use for  $T_0$  is larger than that used by Meiksin & White (2001), to account for the broad lines measured over the full range of line-centre optical depths near  $z = 3.5$  (Meiksin et al. 2001). An effort to calibrate the evolution of  $T_0$  and  $\gamma$  was undertaken by Schaye et al. (2000). The origin of the extra broadening is unknown. A plausible explanation is late He II reionization, but it may be due to turbulence driven by galactic (or star cluster) winds, in which case it may well be present to redshifts as high as 6 or even higher. As we are not concerned with detailed matching to the absorption statistics of particular spectra in this paper, we have not included a complicated evolutionary scenario for  $T_0$  and  $\gamma$ . Instead we simply consider a spread in  $T_0$  by also considering cases with  $T_0 = 10^4 \text{ K}$ , noting that the equation of state is only an approximate description of the IGM temperature and is in any case valid only for overdense regions (Meiksin 1994; Theuns et al. 1998b).

## 2.2 Cosmological model

We consider a flat cosmological model with  $\Omega_{\text{M}} = 0.30$ ,  $\Omega_{\Lambda} = 0.70$ ,  $\Omega_{\text{b}} = 0.041$ ,  $h = H_0/100 \text{ km s}^{-1} \text{ Mpc}^{-1} = 0.70$ , and slope of the primordial density perturbation power spectrum  $n = 1.05$ . The model is COBE normalized, so that the fluctuation normalization at  $z = 0$  in a sphere of radius  $8 h^{-1} \text{ Mpc}$  is  $\sigma_{8h^{-1}} = 0.970$ , and the fluctuation normalization at  $z = 3$  spherically filtered on the scale of the Jeans length for  $T = 2 \times 10^4 \text{ K}$  gas is  $\sigma_J(z = 3) = 1.59$ . The model is consistent with current constraints from the cosmic microwave background (CMB) (Stompor et al. 2001; Netterfield et al. 2002; Pryke et al. 2002), big bang nucleosynthesis (O’Meara et al. 2001), and large-scale structure (Percival et al. 2001; Szalay et al. 2001), as well as the constraint on the size of mass fluctuations on the scale of the Jeans length at  $2 < z < 4$  imposed by the measured flux per pixel distribution of the Ly $\alpha$  forest (Meiksin et al. 2001). We use  $512^3$  particles on a  $1024^3$  mesh in a box of comoving side  $L_{\text{box}} = 25 h^{-1} \text{ Mpc}$ .

## 2.3 Sources of the UV background

We consider two sources of the UV background: QSOs and stellar, such as from LBGs.

We parametrize the QSO comoving luminosity function using the form introduced by Boyle, Shanks & Peterson (1988)

$$\Phi(M, z) = \frac{\Phi^*}{10^{0.4(\beta_1-1)[M^*(z)-M]} + 10^{0.4(\beta_2-1)[M^*(z)-M]}}, \quad (5)$$

where  $M^*(z)$  represents an evolving break magnitude. The results of the 2dF QSO survey show that the QSO counts for  $z < 2.3$  can be acceptably fit by a pure luminosity evolution model in which  $\Phi^*$  is independent of redshift, while the break magnitude evolves according to  $M^*(z) = M^*(0) - 2.5(k_1z + k_2z^2)$ . For  $\Omega_{\text{M}} = 0.3$ ,  $\Omega_{\Lambda} = 0.7$  and  $h = 0.5$ , Boyle et al. (2000) obtain for the  $B$ -band luminosity function  $\beta_1 = 3.41$ ,  $\beta_2 = 1.58$ ,  $\Phi^* = 0.36 \times 10^{-6} \text{ Mpc}^{-3} \text{ mag}^{-1}$ ,  $M_{\text{B}}^*(0) = -22.65$ ,  $k_1 = 1.36$  and  $k_2 = -0.27$ .

At  $z > 2.3$ , the QSO luminosity function is less well determined. We extend the luminosity function to higher redshifts using the results of the SDSS for  $z > 3.5$  (Fan et al. 2001a,b, 2003). The survey limit is too bright to probe to fainter levels than the break, but shows a shallowing in the bright end of the luminosity function to  $\beta_1 = 2.58$ , so that the pure luminosity evolution model may no longer apply at the bright end. Because the pure luminosity model with  $\beta_1 = 3.4$  is ruled out at only the  $2\text{--}2.5\sigma$  level, and possibly only for the brightest QSOs ( $M_{1450} < -27$ ) (Fan et al. 2001a,b, 2003), we consider the pure luminosity evolution case as well. Because, for the values of  $\beta_1$  and  $\beta_2$  we consider, equation (5) predicts that the UV background is dominated by sources with absolute magnitudes near or fainter than  $M^*$ , the contribution of QSOs is poorly constrained by observations. We conservatively assume that the faint end of the luminosity function continues to follow pure luminosity evolution with  $\beta_2 = 1.58$ , and we fix the break luminosity  $M^*(z)$  in equation (5) to match the bright counts measured by the SDSS.

The luminosity function reported by Fan et al. (2001a,b, 2002) is in terms of the absolute magnitude  $M_{1450}$  at  $1450 \text{ \AA}$ . To estimate the contribution of the QSOs to the UV background, we need to convert these values to luminosities at the Lyman edge. We adopt the spectral shape of radio-quiet QSOs as determined at lower redshift by measurements using the *Hubble Space Telescope* (HST) Faint Object Spectrograph (FOS) (Zheng et al. 1997). For  $\lambda < 1050 \text{ \AA}$ , we take  $f_{\nu} \propto \nu^{-1.8}$ , while for  $1050 \text{ \AA} < \lambda < 1450 \text{ \AA}$ , we take  $f_{\nu} \propto \nu^{-0.99}$ . The resulting break values  $M_{\text{L}}^*$  at the Lyman edge for  $\beta_1 = 2.58$  and  $3.41$  are given in Table 1. (The averages over the luminosity function have been performed over the range  $M_{1450} < -18.5$ , and the results adjusted to  $h = 0.7$  for our  $\Lambda$ CDM model.) For  $\beta_1 = 2.58$ , we find the proper emissivity decreases with redshift for  $z \geq 4$  approximately as  $(1+z)^{-1}$ . We also give values for the proper emissivity for  $\beta_1 = 3.2$ . This is less than  $2\sigma$  away from the fits of Fan et al. (2001a) and is able to match the emissivity required to reproduce the measured

**Table 1.** Break luminosity  $M_{\text{L}}^*$  at the Lyman edge and proper emissivity at the Lyman edge required to match the Sloan QSO counts at different redshifts, assuming a QSO luminosity function slope at the bright end of  $\beta_1 = 2.58, 3.20$  and  $3.41$  and a homogeneous UV background. The units of the emissivity are  $10^{26} h \text{ erg s}^{-1} \text{ Hz}^{-1} \text{ Mpc}^{-3}$ .

$z$	$M_{\text{L}}^*$			$\epsilon_{\text{L}}$		
	$\beta_1 = 2.58$	$\beta_1 = 3.20$	$\beta_1 = 3.41$	$\beta_1 = 2.58$	$\beta_1 = 3.20$	$\beta_1 = 3.41$
4	-22.86	-23.98	-24.23	3.23	7.96	9.77
5	-22.11	-23.44	-23.73	2.68	8.19	10.54
6	-21.52	-23.02	-23.35	2.36	8.62	11.52

values of  $\bar{\tau}_\alpha$  for  $4 < z < 6$  using QSO sources alone. For this case, the proper emissivity evolves approximately as  $(1+z)^{1/4}$  for  $z \geq 4$ . We show the resulting comoving QSO luminosity functions at  $z = 6$  for  $\beta_1 = 2.58, 3.20$  and  $3.41$ .

We also consider a possible contribution from LBGs or other stellar sources of Lyman continuum photons. Because UV continuum radiation shortward of the Lyman break is only observed from the brightest LBGs (Steidel et al. 2001), the full contribution of LBGs to the ionizing background is uncertain by a factor of a few for  $z \approx 3$ , and even more uncertain at higher redshifts. The spectral index of the emission, which affects the total ionization rate, is also highly uncertain, depending on the processing of the continuum radiation through the interstellar medium of the galaxy and the IGM, and on the stellar populations of the galaxy. For the estimated ages of  $10^{8 \pm 0.5}$  yr (Papovich, Dickinson & Ferguson 2001), the spectral shape is especially age-sensitive (Fioc & Rocca-Volmerange 1997; Bruzual 2001). For simplicity, we adopt a spectrally flat proper emissivity near the Lyman edge of  $\epsilon_v^{\text{LBG}} \approx 8 \times 10^{27} \text{ h erg s}^{-1} \text{ Hz}^{-1} \text{ Mpc}^{-3}$  at  $z \approx 3$  (Steidel et al. 2001), noting that this estimate was for an Einstein–de Sitter universe, and so overestimates the contribution in the  $\Lambda$ -dominated universes we consider here. The uncertainty in the spectral index introduces an uncertainty in the photoionization rate of 30–50 per cent.

### 3 THE REQUIRED METAGALACTIC EMISSIVITY

Within the context of any given set of cosmological parameters, the flux distribution of the Ly $\alpha$  forest predicted by numerical simulations is fully specified except for one uncertainty: the magnitude of the UV background responsible for the photoionization. Generally, this is fixed by requiring the simulations to reproduce the measured average flux or, equivalently, the mean Ly $\alpha$  optical depth  $\bar{\tau}_\alpha$ . Usually this is done by specifying the required mean photoionization rate  $\Gamma$  per neutral hydrogen atom. In the presence of fluctuations in the UV background, however, the full distribution of  $\Gamma$  should be used, as  $\bar{\tau}_\alpha$  depends non-linearly on  $\Gamma$ . This is particularly important when the distribution is broad. We predict the distribution below and take it into account there. In this section, to simplify the calculation, we assume a constant value of  $\Gamma$  at any given redshift.

The photoionization rate is related to the emissivity of the sources through

$$\Gamma = \int_{\nu_L}^{\infty} d\nu \frac{4\pi J_\nu}{h\nu} \sigma_\nu, \quad (6)$$

where  $J_\nu$  is the angle-averaged intensity of the UV background at frequency  $\nu$ ,  $\sigma_\nu \approx \sigma_L(\nu/\nu_L)^{-3}$  is the photoionization cross-section, and  $\nu_L$  is the frequency at the Lyman edge. The intensity  $J_\nu$  is given by the proper emissivity  $\epsilon_\nu(z)$  of the sources according to (e.g. Meiksin & Madau 1993)

$$J_\nu(z) = \frac{1}{4\pi} \int_z^{z_{\text{on}}} dz' \left( \frac{1+z}{1+z'} \right)^3 \epsilon_{\nu'}(z') \langle \exp[-\tau_\nu(z, z')] \rangle \frac{dl_p}{dz'}, \quad (7)$$

where  $\langle \exp[-\tau_\nu(z, z')] \rangle$  is the average attenuation produced at  $\nu$  due to intervening photoelectric absorption by gas between redshifts  $z$  and  $z'$ ,  $dl_p/dz'$  is the differential proper cosmological line element,  $\nu' = \nu(1+z')/(1+z)$ , and it is assumed that the sources have turned on at some finite redshift  $z_{\text{on}}$ . At high redshift in a flat universe

$$\frac{dl_p}{dz} \approx \frac{c}{H_0} \Omega_M^{-1/2} (1+z)^{-5/2}.$$

Following Zuo (1992b) and Zuo & Phinney (1993), we introduce the attenuation length  $r_0$ , defined by the approximation

$$\langle \exp[-\tau_\nu(z, z')] \rangle \approx \exp[-l_p(z, z')/r_0],$$

where  $l_p(z, z')$  is the proper distance between redshifts  $z$  and  $z'$ . As our simulations do not include the effects of radiative transfer, the full contribution of Lyman limit systems is not accounted for. Their contribution to the total Lyman continuum optical depth from the IGM, however, becomes small compared with that from the Ly $\alpha$  forest itself at the high redshifts we consider here (Meiksin & Madau 1993; Haardt & Madau 1996). As a test of their possible contribution, we replaced the flux in pixels with  $\tau_L > 1$  by zero (fully blackening them), and found this had a negligible effect on the values of  $r_0$  obtained.

It is informative to consider two limiting cases for the contribution of the sources to  $J_\nu$ : (1) absorption limited (AL), for which the attenuation length is much smaller than the horizon; and (2) cosmologically limited (CL), for which the attenuation length much exceeds the horizon. For the AL case, the integral in equation (7) reduces to  $J_\nu = \epsilon_\nu(z)r_0/4\pi$ . For the CL case, attenuation by the IGM is negligible, and the integral is limited by cosmological expansion and the age of the sources (avoiding Olber's paradox). In this case, it is useful to represent the redshift evolution and frequency dependence of the emissivity as power laws:  $\epsilon_\nu(z) = \epsilon_L(1+z)^\eta(\nu/\nu_L)^{-\alpha_S}$ . Using the approximation above for  $dl_p/dz$ , we then obtain  $J_\nu(z) = \epsilon_\nu(z)l_U/4\pi$ , where the effective proper distance in the universe over which sources contribute to  $J_\nu(z)$  is

$$l_U = \frac{c}{H_0 \Omega_M^{1/2}} (1+z)^{-3/2} \frac{1 - [(1+z)/(1+z_{\text{on}})]^{9/2 + \alpha_S - \eta}}{9/2 + \alpha_S - \eta}. \quad (8)$$

As the mean Ly $\alpha$  optical depth constrains the photoionization rate  $\Gamma$  through the simulations rather than the emissivity directly, we re-express these results in terms of  $\Gamma$ . While the above approximations express the magnitude of the emissivity at the Lyman edge, they do not take into account the effect of attenuation at shorter wavelengths in the AL case. The effect of intervening gas is to harden the spectrum, as high-energy photons are able to travel further than photons near the Lyman edge before they are photoelectrically absorbed (Haardt & Madau 1996). We account for the hardening by introducing the metagalactic spectral index  $\alpha_{\text{MG}}$ , which replaces  $\alpha_S$  for the AL case, but not for the CL case. The two limiting cases may then be combined into the approximation

$$\Gamma(z) \approx \frac{\epsilon_L(z)\sigma_L}{h_p(3 + \alpha_{\text{MG}})} r_{\text{eff}}, \quad (9)$$

where  $h_p$  is the Planck constant,  $r_{\text{eff}} = 1/(1/r_0 + 1/l_H)$ , and  $l_H = [(3 + \alpha_{\text{MG}})/(3 + \alpha_S)]l_U$ . The cases AL and CL then correspond to the respective limits  $r_0 \ll l_H$  and  $r_0 \gg l_H$ .

For any pair of  $\epsilon_L$  and  $r_0$ ,  $\Gamma$  is specified through equation (9), and therefore  $\bar{\tau}_\alpha$ . Any pair that yields a desired  $\bar{\tau}_\alpha$ , however, is not necessarily self-consistent. This is because any given value of  $\Gamma$  fixes not only  $\bar{\tau}_\alpha$  but  $\langle \exp(-\tau_L) \rangle$ , and therefore  $r_0$ , as well. It is thus necessary to solve self-consistently for values of  $r_0$  as a function of  $\epsilon_L$ . We show the dependence of  $r_0$  and  $\bar{\tau}_\alpha$  on  $\epsilon_L$  for the results of our  $\Lambda$ CDM simulation in Fig. 2. Here  $\alpha_{\text{MG}} \approx 0$  has been taken to account for the hardening of the radiation field; the associated uncertainty in the amount of hardening, which will also depend on re-emission of Lyman continuum photons by the IGM itself, introduces an uncertainty of 30–50 per cent in the estimates for  $\epsilon_L$ . It is also assumed that the sources have turned on at very high redshifts, so that the limit  $z_{\text{on}} \rightarrow \infty$  may be taken in the expression for  $l_H$ . For small values of  $\epsilon_L$ , the background intensity is attenuation limited

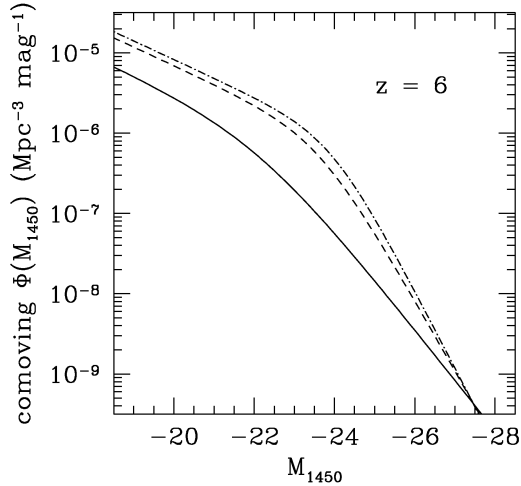


**Figure 1.** The comoving QSO luminosity function at  $z = 6$  for the  $\Lambda$ CDM model with a bright end slope of  $\beta_1 = 2.58$  (solid), 3.20 (dashed), and 3.41 (dot-dashed), with the break magnitude  $M_{1450}^*$  adjusted to match the QSO counts at the bright end measured by the SDSS.

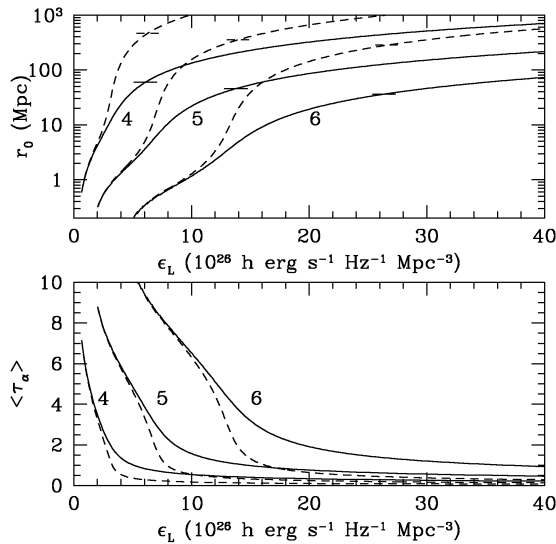


**Figure 2.** The dependence of the attenuation length  $r_0$  (top panel) and mean Ly $\alpha$  optical depth  $\langle \tau_\alpha \rangle$  (bottom panel) on the average emissivity at the Lyman edge for the  $\Lambda$ CDM model at  $z = 4, 5$  and  $6$ , as indicated. It is assumed that the (proper) emissivity evolves according to  $\epsilon_\nu = \epsilon_L(1+z)^{-1}(\nu/\nu_L)^{-1.8}$  for  $z > 4$ , corresponding to QSOs (solid lines) or as  $\epsilon_\nu = \epsilon_L(1+z)^3$ , corresponding to a constant comoving source density (dashed lines). The horizontal bars in the upper panel mark the effective luminosity horizons  $I_H$  of the sources (see text).

(case AL). For large values, the intensity is limited by cosmological expansion (case CL). There is a rapid transition between the two regimes. For the constant comoving density source case, the transition exhibits critical behaviour, with a sudden transition from case AL to case CL as the emissivity is increased: a sufficiently large emissivity drives the attenuation length to such large values that attenuation becomes negligibly important. As attenuation becomes less significant, the mean Ly $\alpha$  optical depth rapidly declines as well. Although the transition is less abrupt for the more gradual QSO evolution case, the ionization structure of the IGM is still very

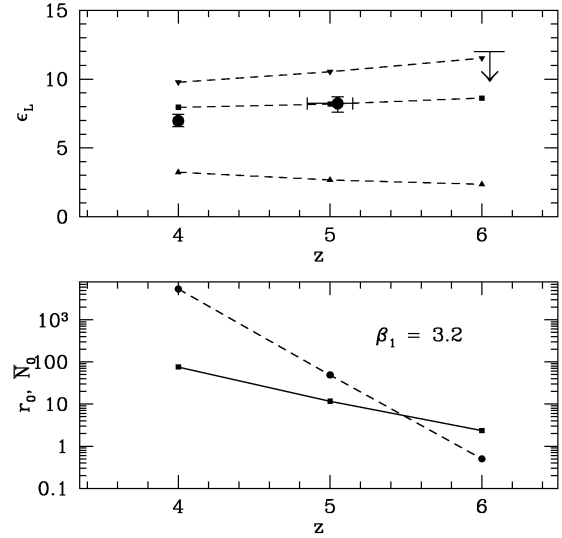


**Figure 3.** Top panel: The emissivity  $\epsilon_L$  at the Lyman edge required to match the measured mean Ly $\alpha$  optical depth  $\bar{\tau}_\alpha$  at  $z = 4, 5$  and  $6$  (Becker et al. 2001; Songaila & Cowie 2002). The units of the emissivity are  $10^{26} h \text{ erg s}^{-1} \text{ Hz}^{-1} \text{ Mpc}^{-3}$ . The estimates based on the  $\Lambda$ CDM model are shown (points), with the error bars corresponding to the redshift ranges and measurement errors on  $\bar{\tau}_\alpha$ . Only an upper limit is shown at  $z = 6$ , corresponding to the measured  $1\sigma$  lower limit on  $\bar{\tau}_\alpha$ . The estimates for the emissivity from QSO sources alone are also shown, for  $\beta_1 = 2.58$  (triangles), 3.20 (squares) and 3.41 (inverted triangles). Bottom panel: The attenuation length  $r_0$ , in proper Mpc (solid line) and the mean number  $\bar{N}_0$  of QSO sources within the attenuation volume (dashed line) predicted by the  $\Lambda$ CDM model are shown for  $\beta_1 = 3.2$ , for which QSOs alone are adequate for providing the UV background at  $z \geq 4$ .

sensitive to the source emissivity. This sensitivity permits a tight bound to be set on the metagalactic emissivity.

We show in Fig. 3 the emissivity required to match the measured values of  $\bar{\tau}_\alpha = 0.73, 2.1$  and  $>5.1$  at the respective redshifts  $z \approx 4, 5$  and  $6$ . We use the results of Songaila & Cowie (2002) for the point at  $z \approx 4$ , estimating the error from the spread in their two fits to  $\bar{\tau}_\alpha$ . The measured values at  $z \approx 5$  and  $6$  are from Becker et al. (2001), with their quoted errors, and only the  $1\sigma$  lower limit is used at  $z \approx 6$  based on Ly $\alpha$  absorption. They set more stringent limits on  $\bar{\tau}_\alpha$  at  $z \approx 6$  using Ly $\beta$  and Ly $\gamma$  absorption, but these are less firm due to absorption modelling uncertainties.

The estimate of  $\epsilon_L$  for LBGs at  $z \approx 3$  (Steidel et al. 2001) exceeds the required value at  $z > 4$  by nearly an order of magnitude. If the proper emissivity were constant out to  $z = 4$ , attenuation by the IGM would become negligible,  $\bar{\tau}_\alpha$  would be driven to very low values and the IGM would become nearly transparent to Ly $\alpha$  photons. Either the proper emissivity of LBGs declines dramatically between  $z \approx 3$  and  $4$ , or the emissivity of LBGs at  $z \approx 3$  has been overestimated. Ferguson, Dickinson & Papovich (2002) argue that indeed the star formation rate in LBGs declines sharply for  $z > 3$ .

The estimated emissivities from QSOs assuming luminosity slopes at the bright end of  $\beta_1 = 2.58, 3.2$  and  $3.41$  are also shown. While QSOs alone are not able to provide the required emissivity for  $\beta_1 = 2.58$ , the preferred value from the SDSS (Fan et al. 2001a,b), QSOs alone are easily adequate for  $\beta_1 = 3.41$ , the value preferred by the 2dF at lower redshift. We find that the predicted QSO emissivity is very sensitive to  $\beta_1$ , scaling roughly as  $\epsilon_L \sim \beta_1^{4.5}$ . The QSO emissivity becomes sufficient for  $\beta_1 > 3.2$  at  $z \geq 4$  within the

errors. The reason for the sensitivity to  $\beta_1$  is that as the luminosity function steepens, the low luminosity QSOs are able to provide an increasing proportion of the total emissivity. While the emissivity above  $M_{1450}^*$  varies little with  $\beta_1$  due to the constraints imposed by the number of QSOs detected at the bright end, the proportion of the total emissivity provided by QSOs fainter than  $M_{1450}^*$  increases from about 50 per cent to nearly 80 per cent as  $\beta_1$  increases from 2.58 to 3.41. For  $\beta_1 = 3.2$ , 75 per cent of the total emissivity is provided by QSOs fainter than  $M_{1450}^*$ . Thus, most of the emissivity is derived from QSOs that are not directly detected. Yet it would seem unlikely that low luminosity QSOs, detected in lower redshift surveys, would disappear altogether. Our estimates are based on the conservative assumption that the faint QSOs continue to follow pure luminosity evolution, although we have no direct evidence for this.

The attenuation length  $r_0$  is predicted to decay exponentially with redshift,  $r_0 \approx 9 \times 10^4 \exp[-1.5(1+z)]$  Mpc for  $4 \leq z \leq 6$  and  $\beta_1 = 3.2$ , as shown in the lower panel of Fig. 3. The mean number  $\bar{N}_0$  of QSOs within the attenuation volume similarly follows an exponential decay,  $\bar{N}_0 \approx 9 \times 10^{12} \exp[-4.35(1+z)]$ , with fewer than a single QSO on average per attenuation volume by  $z = 6$ . If QSOs dominate the UV background, then large fluctuations in the background field and ionization level of the IGM will be introduced for  $z > 5$ . We next turn to the possible role played by a fluctuating background field on the absorption statistics of the IGM.

#### 4 UV BACKGROUND FLUCTUATIONS

The stochastic nature of the discrete sources of the UV metagalactic background will introduce local fluctuations in the intensity of the background. When these sources are sufficiently numerous, the fluctuations will be small. This is expected to be the case for any contribution from galaxies or other stellar sources (e.g. intergalactic star clusters), because of the large number density of these sources. Because of their rarity, however, the contribution from QSO sources will fluctuate at high redshifts. The degree of fluctuation is determined by the number of sources within a photoelectric attenuation volume, the region around the source to which Lyman continuum photons may propagate on average before being photoelectrically absorbed by the IGM.

In order to compute the probability distribution  $f(J)$  of the UV background, we begin by computing the distribution  $f(J, \bar{N})$  of the UV background generated by an average of  $\bar{N}$  sources within a finite sphere of radius  $R$ . Here,  $J$  designates the angle averaged specific intensity of the radiation field at a given frequency and point in space, which we take to be the origin of our coordinate system. (We suppress the frequency subscript to simplify notation.) We work in the Euclidean limit. For any given realization of  $N$  sources with specific luminosities  $L_k$  and distances  $r_k$ ,  $J$  is given by

$$J = \sum_{k=1}^N j_k, \quad (10)$$

where  $j_k = L_k \exp(-\tau_k)/(4\pi r_k^2)$ ,  $\tau_k = r_k/r_0$  is the optical depth due to photoelectric absorption by the IGM, and  $r_0$  is the attenuation length. The distribution of  $J$  is given straightforwardly by the method of characteristic functions (Kendall & Stuart 1969) when the contribution of each source is statistically independent. The characteristic function of  $f(J, N)$  is then (denoting an average over all the sources by  $\langle \dots \rangle$ ),

$$\begin{aligned} \hat{f}(t, N) &\equiv \langle \exp(itJ) \rangle \\ &= \int \exp(it \sum_{k=1}^N j_k) \left[ \prod_{k=1}^N p(L_k, r_k) dL_k dr_k \right]. \end{aligned} \quad (11)$$

Here  $p(L_k, r_k) dL_k dr_k$  denotes the probability of source  $k$  having a specific luminosity in the range  $(L_k, L_k + dL_k)$  and lying within a sphere of radius  $R$  at a distance from the origin in the range  $(r_k, r_k + dr_k)$ . This is given by

$$p(L_k, r_k) dL_k dr_k = \frac{4\pi r_k^2}{(4/3)\pi R^3} \frac{\Phi(L_k)}{\int_{L_{\min}}^{L_{\max}} \Phi(L) dL} dL_k dr_k, \quad (12)$$

and is identical for all the sources. The expression then simplifies to  $\hat{f}(J, N) = I^N(t, R)$ , where, defining  $x = L/L^*$ ,

$$I(t, R) = \int_0^R dr \frac{3r^2}{R^3} \int_{L_{\min}/L^*}^{L_{\max}/L^*} dx \phi(x) \exp(itj). \quad (13)$$

Here we have used equation (12) for  $p(L, r)$  (dropping the subscript  $k$ ), and  $\phi(x)$  is the normalized luminosity function of the sources

$$\phi(x) = \frac{\Phi(xL^*)L^*}{\int_{L_{\min}}^{L_{\max}} \Phi(L) dL}, \quad (14)$$

where  $\Phi(L)$  is the luminosity distribution per unit luminosity and unit (comoving) volume.

Inverting  $\hat{f}(J, N)$  we obtain

$$f(J, N) = \frac{1}{2\pi} \int \exp(-itJ) I^N(t, R) dt. \quad (15)$$

Performing a Poisson average over  $N$  sources with mean  $\bar{N} = (4\pi/3)R^3\bar{n}$ , where  $\bar{n} = \int \Phi(L) dL$ , gives

$$\begin{aligned} f(J, \bar{N}) &\equiv \sum_{N=0}^{\infty} \frac{\bar{N}^N e^{-\bar{N}}}{N!} f(J, N) \\ &= \frac{1}{2\pi} \int \exp(-itJ) \exp\{\bar{N}[I(t, R) - 1]\} dt. \end{aligned} \quad (16)$$

Zuo (1992a) has obtained equation (16) using Markoff's method, although the derivation is more straightforward as shown here. He then presents solutions for the restricted case of an identical luminosity for all sources, no absorption within the attenuation volume ( $\tau_k = 0$ ), and  $R = r_0$ .

It is useful to recast equation (13) using the dimensionless variables  $s = tJ^*$  and  $\tau = r/r_0$ , where  $J^* = L^*/(4\pi r_0^2)$ . The expression for  $I(t, R)$  becomes

$$\begin{aligned} I(s, R) &= \frac{3r_0}{R} \int_0^{R/r_0} d\tau \tau^2 \int_{x_{\min}}^{x_{\max}} dx \phi(x) \exp(isx\tau^{-2}e^{-\tau}) \\ &= \int_{x_{\min}}^{x_{\max}} dx \phi(x) \left\{ \exp[isx(r_0/R)^2 e^{-R/r_0}] \right. \\ &\quad \left. + isx \frac{\bar{N}_0}{\bar{N}} \int_0^{R/r_0} d\tau \exp(isx\tau^{-2}e^{-\tau}) e^{-\tau} (2 + \tau) \right\}, \end{aligned} \quad (17)$$

where  $x_{\min} = L_{\min}/L^*$ ,  $x_{\max} = L_{\max}/L^*$ ,  $\bar{N}_0 = (4\pi/3)r_0^3\bar{n}$  is the average number of sources within an attenuation volume, and we have performed an integration by parts to obtain the final expression.

We may now take the limit  $R \rightarrow \infty$  of equation (17) to obtain

$$\lim_{R \rightarrow \infty} \bar{N} [I(s, R) - 1] = is \bar{N}_0 \int_{x_{\min}}^{x_{\max}} dx x \phi(x) G(sx), \quad (18)$$

where we have defined the function

$$G(\omega) \equiv \int_{\xi=0}^{\infty} d\xi e^{i\omega\xi} \tau^3(\xi), \quad (19)$$

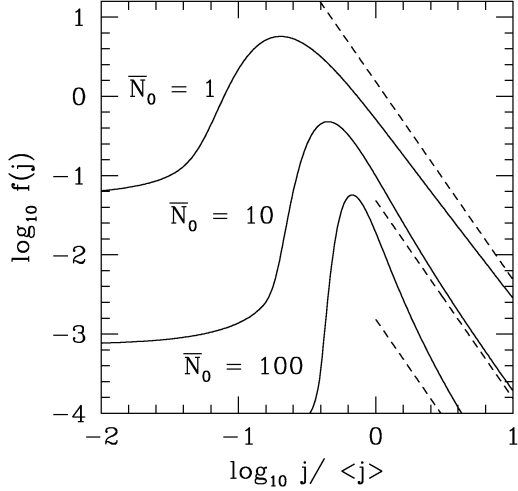


**Figure 4.** The probability density  $f(j)$  for the fluctuations in the intensity  $j$  for  $\bar{N}_0 = 1, 10$  and  $100$  for the QSO luminosity function with  $\beta_1 = 2.58$  and  $\beta_2 = 1.58$  (solid lines). Also shown are the corresponding asymptotic limits  $f(j) \sim \frac{3}{4} \bar{N}_0 \langle x^{3/2} \rangle j^{-5/2}$  (dashed lines). The distributions peak at lower  $j/\langle j \rangle$  for decreasing  $\bar{N}_0$ .

for which  $\tau$  is related implicitly to  $\xi$  through  $\xi = \tau^{-2} e^{-\tau}$ . Using equations (16) and (18), we obtain for the distribution function of  $j = J/J^*$ ,

$$f(j) = \lim_{R \rightarrow \infty} f(J, \bar{N}) J^* \\ = \frac{1}{\pi} \int_0^\infty ds \cos \left[ s \bar{N}_0 \int_{x_{\min}}^{x_{\max}} dx x \phi(x) \operatorname{Re} G(sx) - sj \right] \\ \times \exp \left[ -s \bar{N}_0 \int_{x_{\min}}^{x_{\max}} dx x \phi(x) \operatorname{Im} G(sx) \right]. \quad (20)$$

The leading asymptotic behaviours of the real and imaginary parts of  $G(\omega)$  for  $\omega \ll 1$  are given by

$$\operatorname{Re} G(\omega) \sim \int_0^\infty d\xi \tau^3(\xi) = 3$$

and

$$\operatorname{Im} G(\omega) \sim \int_0^\infty d\xi \sin(\omega\xi) \xi^{-3/2} = (2\pi\omega)^{1/2}.$$

These expressions may be used to derive the leading asymptotic behaviour of  $f(j)$  for  $j \gg 1$ . We obtain  $f(j) \sim \frac{3}{4} \bar{N}_0 \langle x^{3/2} \rangle j^{-5/2}$  ( $j \gg 1$ ), found by rotating the integral over  $s$  in equation (20) into the complex plane and using the method of stationary phase. Here  $\langle x^{3/2} \rangle$  is an average over the luminosity function  $\phi(x)$ . The average value of  $j$  is found directly from equation (16) to be

$$\langle j \rangle \equiv \int_0^\infty dJ (J/J^*) f(J, \bar{N}) = 3 \bar{N}_0 \langle x \rangle (1 - e^{-R/r_0}) \rightarrow 3 \bar{N}_0 \langle x \rangle$$

for  $R \rightarrow \infty$ . Using the asymptotic form for  $f(j)$ , we note that the rms fluctuations of  $j$  diverge at the bright end ( $j_{\max} \gg 1$ ) like  $j_{\max}^{1/4}$ .

In this paper we solve equation (20) numerically using the full QSO luminosity function as determined from observations. We show in Fig. 4 the resulting distributions for  $\bar{N}_0 = 1, 10$  and  $100$ , using equation (5) with  $\beta_1 = 2.58$  and  $\beta_2 = 1.58$ . The peak of the distribution shifts towards lower intensity values as  $\bar{N}_0$  decreases.

## 5 THE LY $\alpha$ FOREST FLUX

### 5.1 The pixel flux distribution

The distribution function of flux per pixel has proven to be an extremely sensitive discriminator between Ly $\alpha$  forest models. The number  $N$  of pixels available in a high-resolution spectrum, such as those from the Keck High Resolution Echelle Spectrometer (HIRES) or the Very Large Telescope (VLT) UV-Visual Echelle Spectrograph (UVES), is of the order of  $10^4$ , so that the cumulative distribution of pixel fluxes may be measured to an rms accuracy of  $\sim N^{-0.5} \approx 0.01$ , although the finite width of the absorption features tends to increase the rms because of the resulting statistical dependence between pixels (Meiksin et al. 2001). We show the pixel flux distributions from the simulations at  $z = 4, 5$  and  $6$  in Fig. 5. Because of the rapidly rising values of  $\bar{\tau}_\alpha$  with redshift, the distributions become increasingly peaked at low flux values.

Fluctuations in the UV background will affect the pixel flux distribution in two ways: a shift in its mean and a tilt in its shape. Matching the measured mean flux to the value predicted for a given set of cosmological parameters fixes the mean  $\Gamma$  for a simulation, so that neglecting fluctuations may lead to a mis-estimate of the mean  $\Gamma$ .

At  $z = 4$ , the number of QSOs in an attenuation volume is sufficiently large that the effects of background fluctuations will be negligible. We therefore only consider the higher redshift cases. We concentrate on the case  $\beta_1 = 3.2$  for the bright end of the QSO luminosity function, as the estimates in Table 1 suggest QSOs alone are able to meet the emissivity requirements to match the measured values of  $\bar{\tau}_\alpha$ .

We show in Fig. 6 (upper panel) the required ionization rates, both with and without the effects of a fluctuating UV background. At  $z = 5$ , the fluctuations have only a small effect on the required  $\Gamma$ , increasing it slightly above the case of smoothly distributed sources, for which  $\Gamma_{-12} = 0.16$ . Once the effect of background fluctuations is included, it is no longer possible for QSOs alone to maintain the ionization of the IGM for  $\beta_1 = 3.2$ ; unless the metagalactic UV spectrum hardens to  $\alpha_{\text{MG}} < 0$ , a small additional smooth

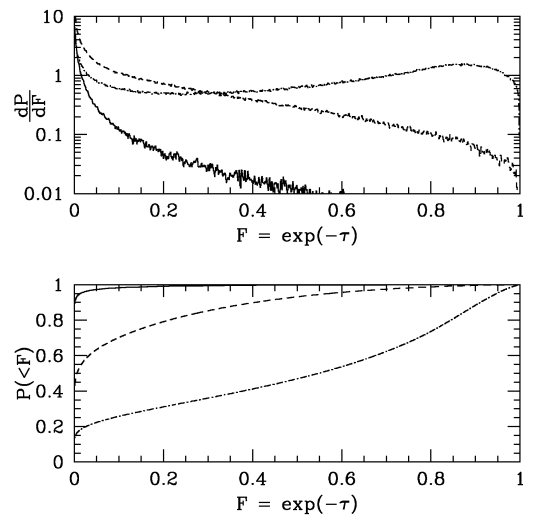


**Figure 5.** Comparison of flux per pixel distributions (top panel) and cumulative flux distributions (bottom panel) at  $z = 4$  (dot-dashed),  $5$  (dashed) and  $6$  (solid), normalized to the measured values of  $\bar{\tau}_\alpha$ . The distributions sharply steepen at vanishing flux levels at high redshift.

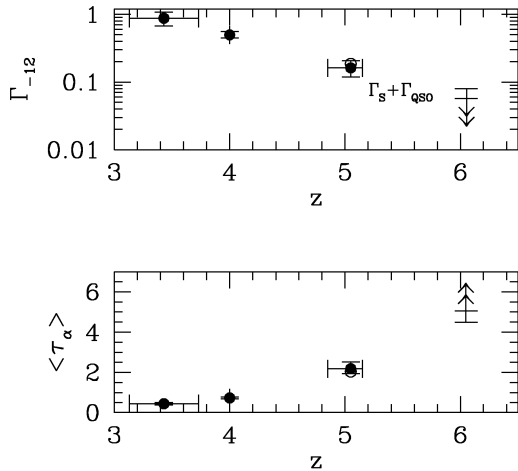


**Figure 6.** Top panel: Estimates for the required mean H I photoionization rate  $\bar{\Gamma}_{-12}$ , in units of  $10^{-12} \text{ s}^{-1}$ , required to match the measured  $\bar{\tau}_\alpha$  at different redshifts. The lowest redshift point is from Meiksin et al. (2001). The solid points are for an assumed homogeneous photoionization background. The open circle at  $z \approx 5$  takes into account fluctuations in the background contributed by QSO sources for  $\beta_1 = 3.2$ , also including a small contribution from a smoothly distributed component. At  $z \approx 6$ , the lower upper limit is for the case of a homogeneous photoionization background. The limit marked  $\Gamma_s + \Gamma_{\text{QSO}}$  includes both a smooth component and the effects of QSO fluctuations for  $\beta_1 = 3.2$ . Bottom panel: The measured  $\bar{\tau}_\alpha$  at different redshifts. The lower points at  $z = 5$  and  $6$  show the values of  $\bar{\tau}_\alpha$  that would result assuming the same mean photoionization rate required from QSOs to match the measured values of  $\bar{\tau}_\alpha$ , but neglecting the effect of the background fluctuations. The fluctuations substantially boost  $\bar{\tau}_\alpha$  at  $z \approx 6$ .

component of  $\Gamma_{s,-12} = 0.025$  must be added. The smooth component is an increase by 15 per cent over the mean QSO ionization rate, a reasonable amount for the diffuse contribution expected to arise from the re-radiation of Lyman continuum photons by the IGM itself. The difference is larger at  $z \approx 6$ . The total ionization rate must now increase from a mean of  $\bar{\Gamma}_{-12} = 0.057$ , to reproduce  $\bar{\tau}_\alpha = 5.1$ , to 0.080, of which  $\sim 40$  per cent is made up of a smoothly distributed component, again reasonable for re-radiation by the IGM. In the lower panel of Fig. 6, a comparison is shown between the measured values of the mean Ly $\alpha$  optical depth and the values that would be obtained assuming the same required mean QSO rates as in the upper panel, but neglecting the role of the background fluctuations. The significant boost of the estimated mean Ly $\alpha$  optical depth by the UV background fluctuations demonstrates the need for taking into account the role of the fluctuations at high redshifts ( $z \gtrsim 5$ ). In particular, this shows that care must be taken in ascribing an abrupt rise in the mean Ly $\alpha$  optical depth to the reionization epoch, as done by Becker et al. (2001), as such a rise may also be due in part to the UV background fluctuations resulting from a small number of sources in an attenuation volume.

We note that the ionization rates in Fig. 6 decay exponentially with redshift from  $z \gtrsim 3.5$ , paralleling the decline in the number counts of QSO sources beyond this redshift.

A comparison of the cumulative distributions of flux per pixel is shown in Fig. 7. We show the differences in the cumulative distributions, as would be used in the Kolmogorov–Smirnov (KS) test. The fiducial models for  $z = 5$  and  $z = 6$  assume a homogeneous UV background. We compare the homogeneous case with the case of  $\beta_1 = 3.2$ , taking into account both the fluctuations in the UV background from the QSOs and the small additional smooth component

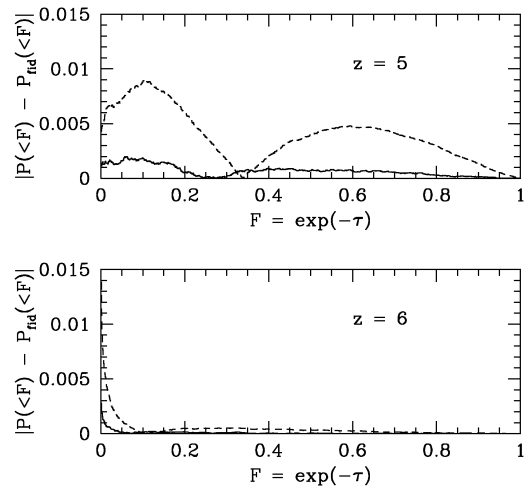


**Figure 7.** Differences of the cumulative distributions of flux per pixel for the  $\Lambda$ CDM simulation with different assumptions for the origin of the photoionization background, at  $z = 5$  (top panel) and  $z = 6$  (bottom panel). The flux distributions are all normalized to the measured values of  $\bar{\tau}_\alpha$ . The cumulative distribution differences are with reference to the fiducial flux per pixel distribution for which a uniform photoionization background is assumed. The solid lines show the difference when fluctuations in a background dominated by QSOs are taken into account, adopting  $\beta_1 = 3.2$ . The dashed lines show the difference assuming  $T_0 = 10^4 \text{ K}$  instead of  $T_0 = 2 \times 10^4 \text{ K}$  for the temperature–density relation, and assuming a homogeneous UV background.

as found above. The effect on the cumulative distributions is small and beyond the current detection limits of the Keck and VLT, except possibly for large sample sizes. The differences, however, may be measurable with a telescope of the extremely large telescope (ELT) class. We also compare the cumulative distributions (for smoothly distributed sources) for two assumptions for the IGM temperature. For the fiducial case,  $T_0 = 2 \times 10^4 \text{ K}$  in equation (4) was assumed. Decreasing  $T_0$  to  $10^4 \text{ K}$  significantly alters the cumulative distribution at  $z = 5$ , although this has a smaller effect at  $z = 6$ . In principle, the uncertainty in the IGM temperature, which corresponds to a change in linewidth of the absorption features, may be corrected for by adjusting the linewidths to match the measured Doppler parameter distribution or wavelet coefficient distribution (Meiksin 2000; Meiksin et al. 2001), so that this uncertainty may not be a limiting factor in detecting the effect of the fluctuations on the pixel flux distribution. We note that lowering the IGM temperature increases the radiative recombination rate and so increases the required ionization rate from  $\Gamma_{-12} = 0.16$  to 0.22 at  $z = 5$  and from  $\Gamma_{-12} = 0.057$  to 0.069 at  $z = 6$ .

## 5.2 Correlations in the UV photoionization background

Zuo (1992b) has shown that the discreteness of the sources of the UV background in the presence of attenuation will result in correlations between the background intensity at points separated in space. His result for the correlation function may be expressed as

$$\xi_J(r) = \frac{1}{3N_0} \frac{\langle x^2 \rangle r_0}{\langle x \rangle^2 r} \int_{r/r_0}^{\infty} du \frac{1}{u} \log \frac{u + r/r_0}{u - r/r_0} e^{-u}, \quad (21)$$

where the averages  $\langle \dots \rangle$  are performed over the dimensionless QSO luminosity function  $\phi(x)$  (equation 14). In Fig. 8, we show the correlation function for  $\beta_1 = 3.2$ , for which nearly the entire UV

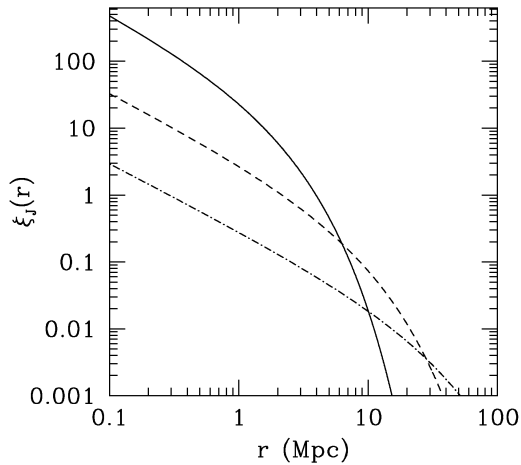


**Figure 8.** The correlation function of the photoionization UV background generated by QSO sources alone assuming  $\beta_1 = 3.2$ , at  $z = 4$  (dot-dashed), 5 (dashed) and 6 (solid).

background may be provided by QSOs. The correlation lengths at  $z = 4, 5$  and  $6$  are  $0.29, 2.2$  and  $4.0$  Mpc (proper), respectively, corresponding to the velocity differences (in the QSO rest frame) of  $125, 1250$  and  $2850$   $\text{km s}^{-1}$ . The background correlations will induce correlations in the pixel fluxes as well, and so serve as a possible means for detecting the discreteness of the sources. The correlations will become diluted by any contribution from a more smoothly distributed component, as may arise from the diffuse background re-radiated by the IGM. We treat the effect of UV background correlations in a separate paper (Meiksin & White, in preparation).

### 5.3 Reionization of the IGM

In this paper, we have considered QSOs as the possible sources that dominate the UV background at  $z \lesssim 6$ . This does not require the QSOs to have initiated the ionization itself, however. The ratio of the Hubble time  $t_H$  to the time for full radiative recombination in our  $\Lambda$ CDM model is

$$t_H n_H \alpha_A \approx 0.024 \left( \frac{\Omega_b h^2}{0.020} \right) (1+z)^{3/2} \left( \frac{\rho}{\bar{\rho}} \right)^{0.65}, \quad (22)$$

where we have used equation (4) and approximated the radiative recombination coefficient as  $\alpha_A \approx 4 \times 10^{-13} (T/10^4 \text{ K})^{-0.7} \text{ cm}^3 \text{ s}^{-1}$ . At  $z = 6$ , the ratio exceeds unity only for  $\rho/\bar{\rho} \gtrsim 3.5$ . At the mean IGM density, the ratio is less than unity for  $z < 11$ . If an early generation of AGN or stars pre-ionized the IGM, for instance, it would be possible for the generation of QSOs at  $z < 6$  to maintain the ionization before the IGM had time to fully recombine. It is none the less interesting to address the question of whether these QSOs would have been sufficient to have performed the reionization as well. The number density of ionizing photons generated by the QSOs over a Hubble time, assuming  $\beta_1 = 3.2$  and  $\eta = 1/4$ , is  $n_\gamma(z) = 6.8 \times 10^{-4} (1+z)^{-5/4} \text{ cm}^{-3}$ . Comparing this with the total number density of hydrogen atoms  $n_H(z)$  gives

$$\frac{n_\gamma(z)}{n_H(z)} \approx 4000 \left( \frac{\Omega_b h^2}{0.020} \right)^{-1} (1+z)^{-17/4}. \quad (23)$$

This crosses unity at  $z = 6.04$ . If these QSOs were responsible for the reionization of the IGM, then they only just could have done so at the highest redshifts to which they have been seen. In the presence

of clumping, reionization by the QSOs becomes problematic. If, however, the IGM is still partially ionized at  $z \approx 6$  following an earlier epoch of reionization, then the QSOs would be adequate for renewing the ionization of the IGM, as the required number of ionizing photons scales like the neutral fraction of hydrogen atoms.

## 6 SUMMARY

We have investigated the dependence of the ionization structure of the IGM at high redshifts ( $z \gtrsim 4$ ) on the emissivity of the sources of the UV photoionization background in the context of a  $\Lambda$ CDM universe. We show that the ionization structure is highly sensitive to the emissivity of the sources at the Lyman continuum edge. For low emissivity values, the intensity of the UV background is limited by the attenuation of Lyman continuum photons by the IGM. For large values of the emissivity, the IGM becomes essentially transparent to Lyman continuum photons, and the UV background is limited instead by cosmological expansion and the age of the sources. We show there is a rapid transition between these two extremes with increasing emissivity. If the UV background is dominated by LBGs at  $z \gtrsim 4$ , then their proper emissivity must dramatically decline from the value estimated at  $z \approx 3$  (Steidel et al. 2001), or they would render the IGM nearly transparent at the Lyman edge and result in a much smaller mean  $\text{Ly}\alpha$  optical depth than measured.

We have also explored the possibility that the UV background is dominated by QSO sources at high redshift. We show that within the observational errors on the high redshift QSO luminosity function, QSOs may provide a substantial component to the UV background, and may even dominate it. If they do dominate, then their sparseness will result in substantial fluctuations in the UV background. We derive the distribution function for the fluctuating intensity in an infinite universe including the effects of attenuation, and show that the distribution significantly broadens for  $z \gtrsim 5$ . The fluctuations in the UV background will increase the estimated  $\text{Ly}\alpha$  optical depth over the value that would be estimated assuming a homogeneous background. This increases the demand placed on the ionization rate required to reproduce a measured mean  $\text{Ly}\alpha$  optical depth and should be taken into account when comparing with estimates of the QSO emissivity. It also shows that care must be taken in attributing a sudden rise in the  $\text{Ly}\alpha$  optical depth to the reionization epoch (Becker et al. 2001), as a sudden rise may result instead from a rapidly decreasing attenuation length and the resulting UV background fluctuations associated with the reduced number of sources that dominate the background. There is a secondary effect of the fluctuations on the pixel flux distribution of the  $\text{Ly}\alpha$  forest, resulting in a small distortion. Although the effect is too small to be measured in a single QSO spectrum from existing facilities such as the Keck or VLT, it may be detectable by combining many spectra, or may need to wait until the arrival of a future generation of ELTs.

The large mean  $\text{Ly}\alpha$  optical depth measured by the SDSS at  $z \approx 6$  (Becker et al. 2001) requires fewer than a single QSO within an attenuation volume on average. This is a significant measurement in that it implies that, if QSOs dominate the UV background, there will be large fluctuations in the mean  $\text{Ly}\alpha$  optical depth from region to region, over spatial scales of  $\sim 4$  Mpc, the expected correlation length of the background radiation field produced by the QSOs at  $z \approx 6$ . This offers a possible means of distinguishing between models for the origin of the UV background dominated by either rare sources such as QSOs, or by relatively more copious sources such as galaxies. We pursue this topic in a companion paper (Meiksin & White, in preparation).

We have also shown that if QSOs dominate the UV background at  $z \approx 6$ , they would just have had sufficient time to provide an adequate number of Lyman continuum photons to ionize the hydrogen, but not at larger redshifts. The estimate, however, is based on the minimal counting requirement of the production of one ionizing photon per hydrogen atom, and neglects the possible role of clumping of the gas. On the other hand, simulations show that much of the volume of the IGM will be underdense and so more readily photoionized. If the IGM were ionized at an earlier phase and had not yet fully recombined by  $z \approx 6$ , then even in the presence of clumping, QSOs may be adequate for renewing the ionization of the IGM. We also note that the UV background fluctuations we expect, if QSOs dominate the ionization of hydrogen, will apply to helium ionization as well, for which it is even more certain that QSOs were the sources of reionization. A complete description of the reionization of the IGM will require accounting for the nature of the ionizing sources, their immediate environments, and the inhomogeneous structure of the IGM. Reviews of recent work in this evolving subject are provided by Madau (2000) and Loeb & Barkana (2001).

In order to match the statistics of observed spectra in detail, it will ultimately be necessary to incorporate radiative transfer into the simulations both to allow for the expected spatial correlations in the UV ionizing background as well as to reproduce the correct gas temperatures (and linewidths), particularly if helium is completely photoionized at only moderate redshifts. Several other physical effects may also be important, such as heating sources in addition to QSOs, or galactic feedback such as winds.

#### ACKNOWLEDGMENTS

The simulations used here were performed on the IBM-SP2 at the National Energy Research Scientific Computing Centre. MW was supported by the NSF, NASA and a Sloan Foundation Fellowship.

#### REFERENCES

- Becker R. H. et al., 2001, *AJ*, 122, 2850  
 Bond J. R., Wadsley J. W., 1997, in Petitjean P., Charlot S., eds, *Structure and Evolution of the Intergalactic Medium from QSO Absorption Line Systems*. Editions Frontières, Paris, p. 143  
 Boyle B. J., Shanks T., Peterson B. A., 1988, *MNRAS*, 235, 935  
 Boyle B. J., Shanks T., Croom S. M., Smith R. J., Miller L., Loaring N., Heymans C., 2000, *MNRAS*, 317, 1014  
 Bruzual G., 2001, *Ap&SSS*, 277, 221  
 Cen R., Miralda-Escudé J., Ostriker J. P., Rauch M., 1994, *ApJ*, 437, L9  
 Croft R. A. C., Hernquist L., Springel V., Westover M., White M., 2002, *ApJ*, 580, 634 (astro-ph/0204460)  
 Fan X. et al., 2001a, *ApJ*, 121, 54  
 Fan X. et al., 2001b, *ApJ*, 122, 2833  
 Fan X., Narayanan V. K., Strauss M. A., White R. L., Becker R. H., Pentericci L., Rix H.-W., 2002, *ApJ*, 123, 1247  
 Fan X. et al., 2003, *AJ*, 125, 1649  
 Ferguson H. C., Dickinson M., Papovich C., 2002, *ApJ*, 569, 65  
 Fioc M., Rocca-Volmerange B., 1997, *A&A*, 326, 950  
 Haardt F., Madau P., 1996, *ApJ*, 461, 20  
 Hernquist L., Katz N., Weinberg D., Miralda-Escudé J., 1996, *ApJ*, 457, L51  
 Hockney R. W., Eastwood J. W., 1988, *Computer Simulation Using Particles*. Adam Hilger, Bristol  
 Kendall M. G., Stuart A., 1969, *The Advanced Theory of Statistics*. Vol. 1. Charles Griffin & Co., London  
 Loeb A., Barkana R., 2001, *ARA&A*, 39, 19  
 Madau P., 2000, *RSPTA*, 358, 2021  
 Meiksin A., 1994, *ApJ*, 431, 109  
 Meiksin A., 2000, *MNRAS*, 314, 566  
 Meiksin A., Madau P., 1993, *ApJ*, 412, 34  
 Meiksin A., White M., 2001, *MNRAS*, 324, 141  
 Meiksin A., Bryan G. L., Machacek M. E., 2001, *MNRAS*, 327, 296  
 Netterfield C. B. et al., 2002, *ApJ*, 571, 604  
 O’Meara J. M., Tytler D., Kirkman D., Suzuki N., Prochaska J. X., Lubin D., Wolfe A. M., 2001, *ApJ*, 552, 718  
 Papovich C., Dickinson M., Ferguson H. C., 2001, *ApJ*, 559, 620  
 Percival W. J. et al., 2001, *MNRAS*, 327, 1297  
 Pryke C., Halverson N. W., Leitch E. M., Kovac, J., Carlstrom J. E., Holzzapfel W. L., Dragovan M., 2002, *ApJ*, 568, 46  
 Schaye J., Theuns T., Rauch M., Efstathiou G., Sargent W. L. W., 2000, *MNRAS*, 318, 817  
 Songaila A., Cowie L. L., 2002, *AJ*, 123, 2183  
 Steidel C. C., Pettini M., Adelberger K. L., 2001, *ApJ*, 546, 665  
 Stompor R. et al., 2001, *ApJ*, 561, L7  
 Szalay A. et al., 2001, preprint (astro-ph/0107419)  
 Theuns T., Leonard A., Efstathiou G., 1998a, *MNRAS*, 297, L49  
 Theuns T., Leonard A., Efstathiou G., Pearce F. R., Thomas P. A., 1998b, *MNRAS*, 301, 478  
 Zhang Y., Anninos P., Norman M. L., 1995, *ApJ*, 453, L57  
 Zhang Y., Anninos P., Norman M. L., Meiksin A., 1997, *ApJ*, 485, 496  
 Zheng W., Kriss G. A., Telfer R. C., Grimes J. P., Davidsen A. F., 1997, *ApJ*, 475, 469  
 Zuo L., 1992a, *MNRAS*, 258, 36  
 Zuo L., 1992b, *MNRAS*, 258, 45  
 Zuo L., Phinney E. S., 1993, *ApJ*, 418, 28

This paper has been typeset from a  $\text{\TeX}/\text{\LaTeX}$  file prepared by the author.